IEEE Photonics Journal
An IEEE Photonics Society Publication

Open Access

Novel Widely Tunable Monolithically Integrated Laser Source

Volume 7, Number 6, December 2015

Sylwester Latkowski, Member, IEEE
Andreas Hänsel
Nandini Bhattacharya
Tjibbe de Vries
Luc Augustin, Member, IEEE
Kevin Williams, Member, IEEE
Meint Smit, Fellow, IEEE
Erwin Bente, Member, IEEE

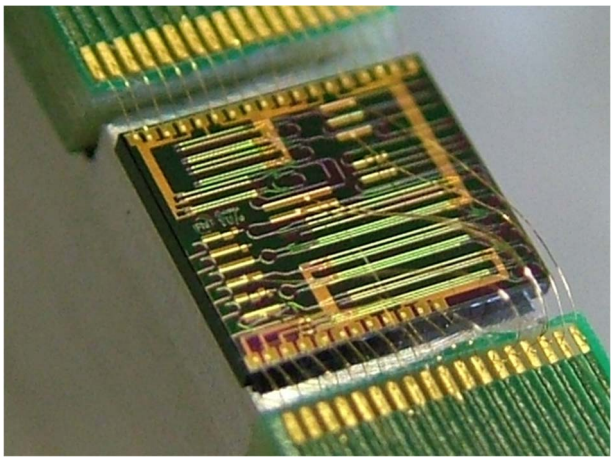

DOI: 10.1109/JPHOT.2015.2493722
1943-0655

IEEE photonics SOCIETY

IEEE

Novel Widely Tunable Monolithically Integrated Laser Source

Sylwester Latkowski,[1] *Member, IEEE*, Andreas Hänsel,[2] Nandini Bhattacharya,[2] Tjibbe de Vries,[1] Luc Augustin,[1,3] *Member, IEEE*, Kevin Williams,[1] *Member, IEEE*, Meint Smit,[1] *Fellow, IEEE*, and Erwin Bente,[1] *Member, IEEE*

[1]COBRA Research Institute, Department of Electrical Engineering, Eindhoven University of Technology, 5600 Eindhoven, The Netherlands
[2]Optics Research Group, TU Delft, 2628 Delft, The Netherlands
[3]SMART Photonics, 5612 Eindhoven, The Netherlands

DOI: 10.1109/JPHOT.2015.2493722

Manuscript received September 29, 2015; revised October 15, 2015; accepted October 17, 2015. Date of publication October 26, 2015; date of current version November 2, 2015. This work was supported by the Technology Foundation STW under the Project 11360 LWAVE-TECH and the NRC Photonics program. Corresponding author: S. Latkowski (e-mail: s.latkowski@tue.nl).

Abstract: We report a novel type of monolithically integrated tunable semiconductor laser. The tuning is achieved by three intracavity Mach–Zehnder interferometers, realized in passive waveguides and using voltage-controlled electro-optic phase modulators requiring only four control voltages. The potential of the design is demonstrated by a realized laser system that shows an optical linewidth of 363 kHz, output power of 3 mW, and a record tuning range of 74.3 nm. Such a continuous wavelength span is in excess of any monolithic semiconductor laser reported up to date. Precision of the tuning mechanism is demonstrated by a scan over a 0.89-GHz-wide absorption line of acetylene. The laser design is suitable for a number of applications, including gas spectroscopy, telecommunication, and optical coherence tomography. The laser has been fabricated in a multi-project wafer run on an indium phosphide-based generic photonic foundry platform and demonstrates the potential of these technology platforms.

Index Terms: Semiconductor laser, tunable laser, photonic integrated circuit.

1. Introduction

For applications such as optical gas sensing of multiple gas species, a widely tunable single longitudinal mode laser is desirable. This is particularly true when there is background interference from other unknown gas species. The laser should be able to scan precisely over an individual absorption line that typically has a linewidth in the order of few gigahertz and should offer a wide range of accessible wavelengths in order to cover many species. Several approaches to a widely tunable, monolithic semiconductor laser have been demonstrated, which in most cases target telecommunications oriented applications. Sampled grating based, distributed Bragg feedback (SG-DBR) type of lasers proposed by Mason *et al.* [1] offer quasi-continuous access to the tuning range with the widest range demonstrated being 72 nm by Jayaraman *et al.* [2]. The performance of this type of devices relies strongly on the quality of the fabricated gratings and, therefore, requires demanding lithography techniques. Over 100 nm wavelength span covered by a superstructure grating (SSG-)DBR lasers was demonstrated by Tohmori *et al.* [3] Although it is the widest tuning range reported, it included multi-mode operation regions, and the

reported range of 86 nm for single-mode operation was not completely accessible. A mode-hop free tuning over 65 nm was demonstrated by Suzuki *et al.* [4] with a monolithic semiconductor laser structure comprised of a lateral-grating-assisted lateral-co-directional-coupler (LGLC) and SG-DBR. Khan and Cassidy [5] have also demonstrated a tuning capability of around 100 nm using a coupled-cavity approach [6] and an asymmetric multi-quantum-well based active core. The full tuning range was however achieved with a cleaved-couple-cavity (C^3) configuration in which the laser cavity is formed by two separated chips. A monolithic chip version of the device with a focused ion beam milled feature reached up to 60 nm tuning. Gierl *et al.* [7] presented a continuous tuning range of 102 nm using an external cavity approach based on a vertical-cavity surface-emitting laser (VCSEL) with the wide tuning range achieved by a micro-electro mechanical actuation of a dielectric mirror membrane. Despite the devices architecture being suitable for on-wafer mass production, it is not a monolithic or monolithically integrated semiconductor chip. In the group of multi-branch type of lasers [8] or Y-branch lasers [9]–[12] a widest tuning range of 45 nm was demonstrated with a Y3-branch structure by Kuznetsov and co-workers [13]. This device does not rival the record values reported and mentioned above, but it is worth mentioning that its wavelength selection mechanism has a similar operating principle to the one presented in this paper, even though it requires a more complex tuning control system than the one that is demonstrated here. Fabrication difficulties of the Y3-branch led to a discontinuous tuning wavelength range with inaccessible spectral gaps. An arrayed waveguide based tunable laser, operating at wavelengths around 1.7 μm has been developed by Tilma *et al.* [14] for application in optical coherence tomography systems. In this case the intracavity filter was tunable over 160 nm [15] but the laser was tunable for only 60 nm. More recently, a number of tunable lasers realized using hybrid III-V on Silicon integration technologies were reported, offering tuning ranges of 40 nm [16] and 45 nm [17]. Here, we report an integrated extended cavity ring lasers with a widely tunable intra-cavity wavelength filter and a simple control mechanism. The wavelength selection is based on a sequence of Asymmetric Mach–Zehnder Interferometers (AMZI) that are tuned using voltage controlled electro-refractive phase modulators (ERM). Such a design is shown to have potential for a wide and continuous wavelength tuning while using only four control signals. Furthermore, the voltage operated ERMs offer increased speed (up to several GHz in the current technology on n-doped substrate), low power ($<$ 10 μW DC) and no heat related response time when compared to current or thermally controlled electro-optic modulators or grating based tuning elements. Two generations of AMZI based tunable lasers have been designed and realized in Multi-Project Wafer (MPW) runs in the indium phosphide (InP) based generic photonic integration technology platform developed at the COBRA Research Institute [18] and presently operated commercially by SMART Photonics [19] as one of the three JePPIX [20] InP platforms. The fabricated lasers operate in a wide range centered around 1.52 μm wavelength. Characterization shows that single-mode (longitudinal) operation with a side-mode suppression ratio (SMSR) of more than 30 dB and a wide tuning range of 74.3 nm can be achieved. This scan range is wider than that of any monolithically integrated, widely tunable laser demonstrated up to date. The spectral range covered by the laser allows for monitoring of several gas species which are attractive from medical and industrial applications point of view, for example, ammonia (NH_3), hydrogen cyanide (HCN), diethylamine ($C_4H_{11}N$), dimethylamine ($(CH_3)_2NH$), and methylamine (CH_3NH_2). Using this laser, we could observe a 0.89 GHz wide single absorption line of acetylene ($^{12}C_2H_2$) with 6 MHz (48 fm) steps demonstrating its capabilities for accurate scanning of the wavelength and its applicability for single line gas spectroscopy. Furthermore, an excellent agreement of experimental results with simulations and design objectives [21]–[23] was obtained.

2. Laser Geometry

An integrated extended ring cavity laser as schematically depicted in Fig. 1(a) is used. It is composed of several basic building blocks available in the integration technology platform [18]. A semiconductor optical amplifier (SOA) provides optical gain, a tunable optical band-pass filter

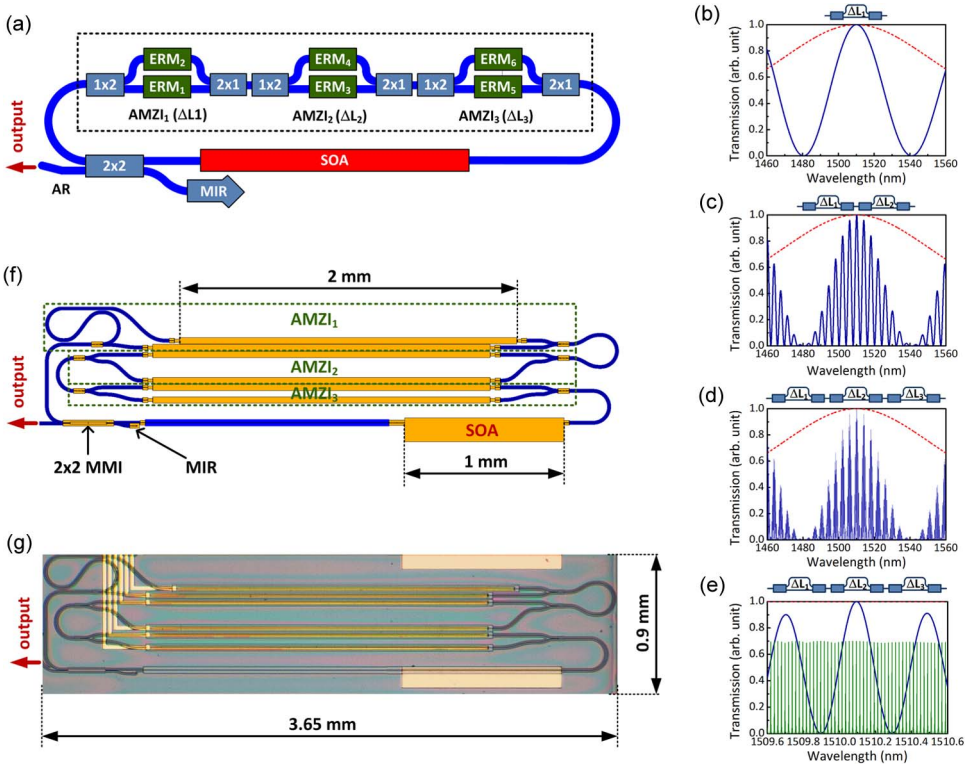

Fig. 1. (a) Schematic of the extended cavity ring laser with an intra-cavity wavelength filter consisting of a three AMZI stages (dashed box), an SOA, a 2 × 2 MMI coupler used for coupling out the optical signal in both directions, and a multimode interference reflector (MIR) connected to one of the outputs that ensures uni-directional operation of the laser and passive waveguides connecting all components. (b)–(e) The transmission spectra of the wavelength filter in blue overlapped with the gain profile indicated in red. (b) Single AMZI stage; (c) two AMZI stages in series; (d) three AMZI stages in series; (e) three AMZI stages in series over the wavelength span of 1 nm overlapped with longitudinal cavity modes in green. (f) Mask layout of the device with building blocks colored in yellow and passive waveguides in blue. (g) Microscope photograph of fabricated PIC with one extended cavity ring laser.

(indicated by the dashed box) formed by multimode interference couplers (MMI) and ERMs, an on-chip multimode interference reflector (MIR), and straight and curved passive waveguides connect all components.

The wavelength selective filter is fully realized using passive waveguide components and it comprises three tunable AMZI stages in series. The transmission of an individual AMZI is periodic with respect to the frequency with a free spectral range FSR $= c/\Delta L_N$ where c is the speed of light in vacuum and ΔL_N the optical path length unbalance of N-th filter stage. The unbalanced interferometric configuration enables a tuning mechanism in which a change of the optical phase by 2π between the arms tunes the filter over one full FSR of the AMZI. The physical length of the optical waveguides in the arms can be defined on a sub-micrometer (0.7 μm) scale using contact lithography. Voltage controlled ERMs with efficiency of 15°/V·mm are available in the integration technology platform used [18]. Using this technology AMZI based filters with a tuning range in the order of a few tens of nanometers (a few terahertz) can be realized [11], [24]. A single AMZI stage features a sinusoidal transmission profile, as schematically depicted in Fig. 1(b), where its transmission is overlapped with the spectral gain profile of the SOA. This in combination with the fundamental mode structure of the laser cavity is not sufficient to achieve single mode operation. The selectivity of such a filter can be improved by combining several identical AMZI in series, or using a sequence of AMZIs with varying path-length unbalances $(\Delta L_1 \neq \Delta L_2 \neq \Delta L_3)$ as shown in Fig. 1(c) and (d) for two and three stage filter. This will allow one to select the required

longitudinal mode of the ring laser cavity, as depicted in Fig. 1(e), where the three stage based filter transmission is overlapped with the longitudinal cavity modes over a narrow range (0.8 nm) around the transmission peak. In the geometry with the three stage filter, the unbalances $\Delta L_{1,2,3}$ should be selected to allow for only one maximum within the gain curve of the amplifier. The coarse tuning AMZI stage (smallest ΔL_N) controls tuning on the scale of SOA gain profile, while the longitudinal cavity mode selection is governed by the two remaining AMZI stages. Cold cavity analysis of the laser including the spectral shape of the gain profile shows that at least 4% power loss of all ring cavity modes other than the selected mode can be achieved, which is sufficient for a good mode selectivity. Therefore the steady state SMSR of the laser above threshold can be predicted, following the method discussed by Coldren *et al.* [25], to be around 23 dB at an SOA current injection of 2.5 times the lasing threshold value. A relatively simple tuning scheme can be applied when ERMs of equal lengths are used in the AMZI stages. The equal lengths of the ERMs imply that (assuming identical performance of each ERM) the same control signal $S_{2\pi}$ is required in order to achieve a phase delay of 2π in each stage of the filter. Furthermore, as the unbalances $\Delta L_{1,2,3}$ are fixed, a simple linear relationship between the change in control signals $\Delta S_{1,2,3}$ and the frequency detuning Δf of the series of three AMZIs can be derived:

$$\Delta S_N(f) = \frac{\Delta f}{v_g(f)} S_{2\pi}(f) \Delta L_N \tag{1}$$

with $N = 1, 2, 3$, and v_g being the group velocity. From the relationship given by (1), a set of ΔS_N control signals within $S_{2\pi}$ can be calculated to allow for continuous frequency tuning of the filter over its full FSR. It has to be noted that the group velocity and $S_{2\pi}$ and consequently ΔS_N are frequency dependent. These chromatic dispersion effects have to be taken into account when addressing a wide tuning range with high accuracy. It should be noted that in principle only one ERM is required in each AMZI stage to continuously tune the filter. However, to continuously tune the laser, the cavity modes also have to be tuned, and for this, an in-line phase modulator should be added, or at least one AMZI stage should contain the ERMs in both arms. In addition, since the precise unbalance cannot be controlled in manufacturing, it is more convenient for calibration purposes to have an ERM in each AMZI arm, as shown in the Fig. 1(a). Therefore, an additional control signal needs to be applied to a fourth ERM (in principle any of the available ones not used in tuning the filters transmission spectrum) which enables the in-line cavity phase adjustments and therefore allows for continuous tuning of the laser system, providing that the voltage transitions at the 2π wrapping points are executed sufficiently fast, i.e. faster than the build-up time of the cavity modes of several ns. This is technically feasible with the voltage controlled ERMs [18], [26], [27]. As the phase change during tuning over the full range covers many times 2π, the control signals on the phase modulators to tune the laser have to be applied modulo 2π (ΔS_N), which means that they have to be switched back by 2π when they become too large.

3. Simulations

Full circuit level time domain simulations of the laser using in-house [28] as well as a commercially [29] available software packages show that side-mode suppression ratios in excess of 30 dB can be achieved at any operation point lying within the 40 nm of the SOAs 3 dB gain bandwidth, as depicted in Fig. 2(a) and (b).

An example of a simulation result showing single mode operation is presented in Fig. 2(a). The envelope of the three stage AMZI filter transmission spectrum can be recognized. The spectrum near the lasing wavelength with neighboring cavity modes at FSR of 0.05 nm (5 GHz) is presented in the inset showing an SMSR of more than 40 dB. The results obtained from several simulations for different settings of the voltages applied to one of the phase shifters in the coarse AMZI stage of the filter are presented in Fig. 1(b), where the spectra from the simulations have been overlapped. It shows a tuning range over 40 nm around the gain peak of the amplifier used in the simulations.

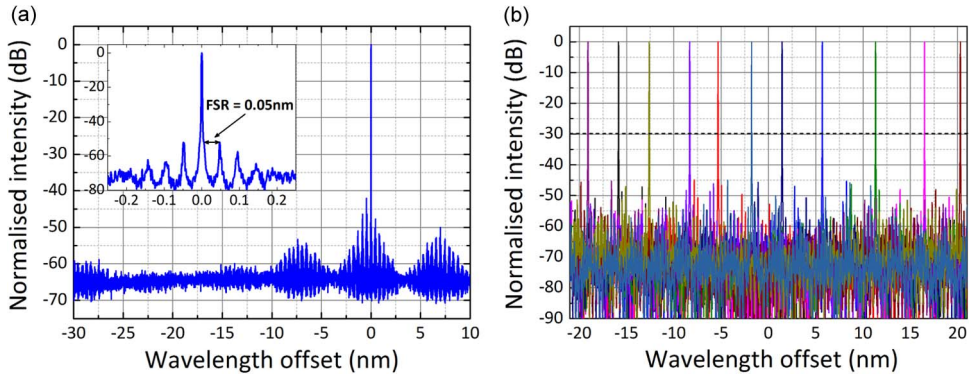

Fig. 2. Spectral output predicted by a photonic circuit simulator [29] for a PIC-based ring laser. (a) High-resolution simulation output showing single-mode operation with the output spectrum around the lasing mode presented in the inset. (b) Several low resolution (due to reduced time of simulations) output spectra obtained for different sets of voltages applied to the phase modulators with constant temperature and current injection into the SOA section.

4. Photonic Integrated Circuit

The laser presented in the previous section was designed and fabricated using a generic active-passive integration technology platform developed at the COBRA Research Institute and currently available for external users via foundry services offered by SMART Photonics [19]. Within this technology platform a limited set of basic building blocks (BB) is available, which can be combined in various topologies to form complex photonic integrated circuits [18]. Depending on their main function these BBs are allocated on either an optically active or a passive epitaxial layer-stack section grown on the InP substrate. The active layer stack is capable of on-chip light generation, amplification and absorption. The passive layer stack provides low optical loss wave guiding with losses being typically between 1 and 2 dB/cm for shallow etched waveguides and from 3 to 5 dB/cm for deeply etched waveguides which offer a smaller minimum bend radius (75 μm). These functionalities are guaranteed in the C-band (1530–1565 nm). The mask layout of the laser was designed using the OptoDesigner package from Phoenix Software [30]. A mask set including structures corresponding to the extended cavity ring laser was designed as depicted in Fig. 1(f). The optical gain is provided by a 1 mm long semiconductor optical amplifier based on a 4 InGaAs quantum-well (QW) active core. A 2 $\times$ 2 MMI coupler is used for coupling out of the laser cavity in both clockwise and counter-clockwise directions. One of the outputs is connected to a Multi-Mode Interference Reflector (MIR) assuring a uni-directional operation of the laser with the output signal available on the second 2 $\times$ 2 MMI port. The tunable, intra-cavity optical band-pass filter consists of three individual AMZI stages each formed by two 2 $\times$ 1 MMI couplers, deeply etched passive waveguides, and a 2 mm long ERM section (with a $V_{2\pi} = -11.5$ V) in each branch to allow for wavelength tuning and calibration. The ring cavity is formed by connecting all components with deeply etched passive waveguides and features an overall average physical length of $L_R = 16$ mm, which corresponds to a cavity mode spacing of 5.4 GHz. The internal laser loss can be attributed to the passive losses in the extended cavity. The total passive loss in the laser cavity of 8 dB can be calculated taking into account the overall lengths of deep and shallow waveguides including the ERM sections, number of MMIs (typical insertion loss of 0.5 dB each) and assuming an average loss value for each type of the waveguide. The optical signal is routed to the edge of the chip using a shallow etched waveguide. In order to reduce the intensity of back-reflection from the facet as much as possible, this waveguide ends at a 7° angle with respect to the normal to the cleaved edge of the chip, and the facet is anti-reflection coated. The physical path length unbalances ΔL_1, ΔL_2 and ΔL_3, were selected to be 1263 μm, 97 μm and 9 μm corresponding to free spectral ranges of 66 GHz, 0.9 THz and 9 THz for $AMZI_1$, $AMZI_2$ and $AMZI_3$ as indicated in Fig. 1(f). The $AMZI_3$ with the smallest FSR determines the

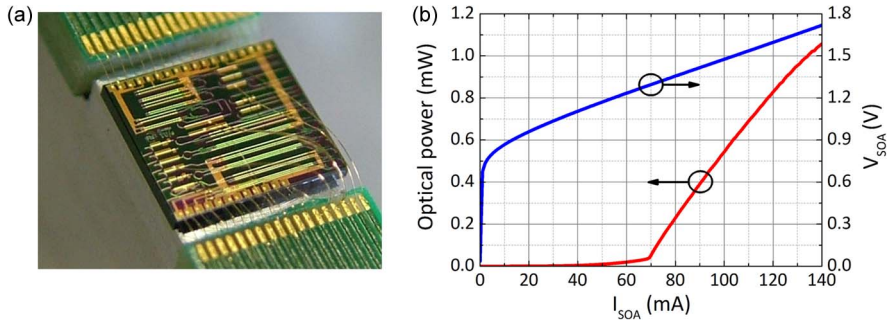

Fig. 3. (a) Fabricated photonic integrated circuit with dimensions 4.7 × 4.1 mm, containing six variants of such a laser and several additional test structures. The chip is mounted on an aluminum evaluation platform and wire-bonded to distribution printed circuit boards. (b) LVI characteristics of the laser. The optical power (red) is measured in a (lensed) fiber with a typical coupling loss of ~5 dB; the voltage drop across the SOA section (blue) indicates a slope resistance of 5.36 Ω.

side mode suppression ratio with the neighboring cavity modes. The two other AMZIs suppress the other transmission maxima of $AZMI_3$ and assure that only one maximum fits into the gain curve of the SOA section. Such a combination of the AMZIs allows for a wide tuning range while maintaining single-mode operation. A micrograph of an area of the fabricated chip including the tunable laser is shown in Fig. 1(g).

5. Experimental Results

The fabricated chip was mounted on an aluminum sub-mount and the electrical contacts of ERMs and SOA were wire-bonded to electrical signal distribution PCBs for ease of control and characterization, as shown in Fig. 3(a). The sub-mount is temperature stabilized at 18 °C with a passive water cooling system. The optical signal is collected with an anti-reflection coated lensed fiber (OZ-optics TSMJ-EA-1550-9/125-0.25-7-2.5-14-1-AR) and fed with a standard single mode fiber to the measurement equipment via an optical isolator (OFR IO-H-1550-0814). The forward bias current injection into the SOA section was supplied from a laser diode controller (Thorlabs PRO8000/LDC8005) and two voltage source modules (National Instruments: NI9269 and NI9923 modules in cDAQ-9178 chassis) were used to reverse bias and control the ERM sections. A threshold current $I_{th} = 68$ mA has been measured as shown in Fig. 3(b). The slope resistance is $R_{SL} = 5.36\ \Omega$ (specific contact resistance of $5.36 \cdot 10^{-9}\ \Omega \cdot m^2$). Single-mode operation with an SMSR of 43 dB at a bias current $I_{SOA} = 134$ mA has been achieved as depicted in Fig. 4(a). The high resolution optical spectrum analyzer (APEX Technologies 2041A) was used to record the spectral data with resolution of 20 MHz allowing to resolve the laser cavity modes as presented in the inset of Fig. 4(a). The spectral properties are in good agreement with the simulations based on the design values, as depicted previously in Fig. 2(a). A delayed self-heterodyne (SH) setup following the original one proposed by Okoshi *et al.* [31] was used to measure the optical linewidth. The SH set-up consisted of a LiNbO based phase modulator and a 25 km long SMF based delay line was connected to a fast photodiode (u2T-XPDV-1020R) and an electrical spectrum analyzer from Agilent (E4448A) with the following settings for measurements: resolution bandwidth (RBW) 10 kHz, video bandwidth (VBW) 1 kHz and the sweep time (ST) of 1.9 s. The RF spectrum presented in Fig. 4(b) has been recorded with the laser operated at the same biasing conditions as used previously for the single mode operation and shows an optical linewidth of 363 kHz (FWHM measured from the Lorentzian fit). The reported value of the optical linewidth compares well with the optical linewidths reported from other widely tunable laser sources, being typically in the range from 300 kHz to 2 MHz the case of SG-DBR [32] or DS-DBR [33], [34].

The wavelength tuning range was investigated by applying reverse voltages in the range from 0 V to $V_{2\pi} = -11.5$ V to each of the three ERMs: one in each of the AMZI stages of the

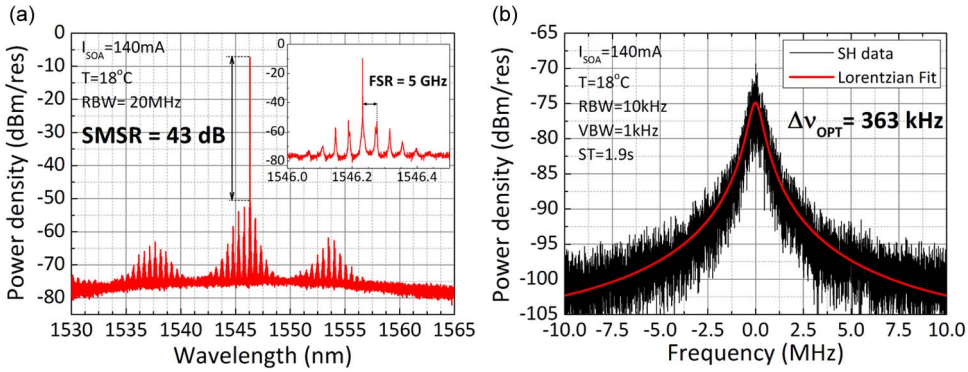

Fig. 4. Characteristics of the fabricated device. (a) High-resolution (20 MHz) optical spectrum showing continuous wave and single-mode operation with a side mode suppression ratio of 43 dB; the inset presents an expanded view of the lasing mode, and neighboring cavity modes are spaced at 5.4 GHz. (b) Optical linewidth of the lasing mode of 363 kHz has been measured using a delayed self-heterodyne (SH) method. Measurement data and Lorentzian fit are indicated in black and red, respectively.

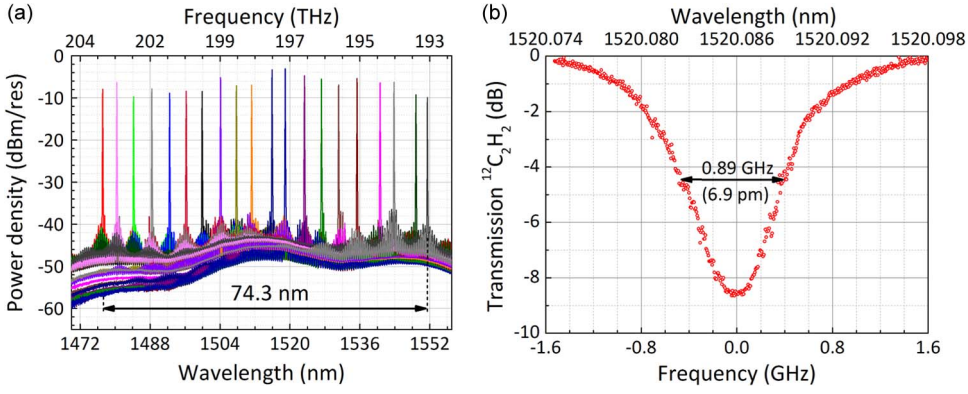

Fig. 5. (a) Twenty overlapped optical spectra (0.05 nm resolution) recorded with the SOA section DC biased at $I_{SOA} = 140$ mA (~2.2 times of the I_{th}) at room temperature, showing a tuning range of 74.3 nm. (b) A 0.89 GHz wide absorption line of acetylene (R-branch 9th line) measured with the laser tuned by applying a series of reverse bias voltages to the ERM phase sections with the amplifier current I_{SOA} set at 125 mA.

band-pass filter while the SOA section bias current was kept constant at $I_{SOA} = 140$ mA. The remaining phase shifters were grounded. Resulting optical spectra recorded with a standard resolution (0.05 nm) optical spectrum analyzer (Yokogawa AQ 6375) at 20 different sets of voltages applied to the three ERMs are overlapped and shown in Fig. 5(a). A wavelength tuning range of 74.3 nm (9.6 THz) around 1525 nm is demonstrated. To our best knowledge this is the widest tuning range reported for monolithically integrated tunable lasers to date. Fine tuning of the laser using the AMZI based filter is demonstrated by recording the absorption spectrum of a single absorption line of acetylene. For a gas detection experiment, the optical signal from the isolator was split into two branches: one used as a reference for recording any optical power fluctuations and the other one sent through a reference acetylene cell (Thorlabs CQ09050-CH12: $^{12}C_2H_2$, 50 torr, 5 cm). Both branches were followed by the optical power meters (Agilent 81636B photodetector module and Newport 1835-C with free space photodiode head). For the wavelength range calibration optical spectra were recorded with the high resolution optical spectrum analyzer with a resolution of 20 MHz (APEX Technologies AP2041A). The transmission profile of the R-branch 9th line of acetylene [35] recorded using the extended cavity ring laser is shown in Fig. 5(b). The absorption spectrum was recorded at 500 points with steps of 6.27 MHz (48 fm)

performed by applying a consecutive sequence of sets of reverse voltages to the four ERMs, while the SOA bias and temperature of the chip were constant during the experiment. The measured absorption line features a linewidth of 0.89 GHz (6.9 pm).

6. Conclusion

We have demonstrated a fully integrated widely tunable ring geometry laser with an intra-cavity wavelength filter based on AMZIs. The photonic integrated circuits operating at from 1475 nm to 1550 nm were realized using the monolithic InP active-passive generic integration technology platform developed at the COBRA Research Institute. Two sets of chips were designed and fabricated: a first set at the COBRA Research Institute and a second set via foundry services offered by SMART Photonics through JePPIX. The two sets of devices show very similar performance. The experimental results presented show a very good agreement with the simulations performed either using in-house developed software or a commercially available photonic circuit simulator package. The demonstrated tunable laser geometry provides 3 mW (ex-facet) of output power, single-mode operation, an optical linewidth of 363 kHz, and a continuous tuning potential over the range of 74 nm; such performance rivals the state-of-the-art offered by other monolithic devices reported up to date. Output power can be further increased by integrating a booster amplifier. The feasibility for use in single line gas spectroscopy systems by providing precise wavelength tuning was validated in a gas detection setup. The use of voltage controlled ERMs as tuning elements is advantageous over the current controlled alternatives in terms of tuning speed and accuracy. The design can be easily transferred to other foundry platforms and scaled to operate at another wavelength range. These aspects vastly broaden the scope of potential applications of the demonstrated design.

References

[1] B. Mason, J. Barton, G. Fish, L. Coldren, and S. P. DenBaars, "Design of sampled grating DBR lasers with integrated semiconductor optical amplifiers," *IEEE Photon. Technol. Lett.*, vol. 12, no. 7, pp. 762–764, Jul. 2000.

[2] V. Jayaraman, A. Mathur, L. Coldren, and P. Dapkus, "Extended tuning range in sampled grating DBR lasers," *IEEE Photon. Technol. Lett.*, vol. 5, no. 5, pp. 489–491, May 1993.

[3] Y. Tohmori *et al.,* "Over 100 nm wavelength tuning in superstructure grating (SSG) DBR lasers," *Electron. Lett.*, vol. 29, no. 4, pp. 352–354, Feb. 1993.

[4] T. Suzuki *et al.,* "Wide-tuning (65 nm) semi-cooled (50 °C) operation of a tunable laser based on a novel widely tunable filter," in *Proc. IEEE OFC/NFOEC*, Mar. 2011, pp. 1–3.

[5] F. K. Khan and D. T. Cassidy, "Widely tunable coupled-cavity semiconductor laser," *Appl. Opt.*, vol. 48, no. 19, pp. 3809–3817, Jul. 2009.

[6] K. J. Ebeling, L. A. Coldren, B. I. Miller, and J. A. Rentschler, "Single-mode operation of coupled-cavity GaInAsP/InP semiconductor lasers," *Appl. Phys. Lett.*, vol. 42, no. 1, pp. 6–8, Jan. 1983.

[7] C. Gierl *et al.,* "Surface micromachined tunable 1.55 μm-VCSEL with 102 nm continuous single-mode tuning," *Opt. Exp.*, vol. 19, no. 18, pp. 17336–17343, Aug. 2011.

[8] S. Miller, "Multibranch frequency-selective reflectors and application to tunable single-mode semiconductor lasers," *J. Lightw. Technol.*, vol. 7, no. 4, pp. 666–673, Apr. 1989.

[9] M. Schilling *et al.,* "Asymmetrical Y laser with simple single current tuning response," *Electron. Lett.*, vol. 28, no. 18, pp. 1698–1699, Aug. 1992.

[10] M. Schilling *et al.,* "Widely tunable Y-coupled cavity integrated interferometric injection laser," *Electron. Lett.*, vol. 26, no. 4, pp. 243–244, Feb. 1990.

[11] M. Kuznetsov, P. Verlangieri, A. Dentai, C. Joyner, and C. Burrus, "Asymmetric Y-branch tunable semiconductor laser with 1.0 THz tuning range," *IEEE Photon. Technol. Lett.*, vol. 4, no. 10, pp. 1093–1095, Oct. 1992.

[12] M. Kuznetsov, "Design of widely tunable semiconductor three-branch lasers," *J. Lightw. Technol.*, vol. 12, no. 12, pp. 2100–2106, Dec. 1994.

[13] M. Kuznetsov, P. Verlangieri, A. Dentai, C. Joyner, and C. Burrus, "Widely tunable (45 nm, 5.6 THz) multi-quantum-well three-branch Y3-lasers for WDM networks," *IEEE Photon. Technol. Lett.*, vol. 5, no. 8, pp. 879–882, Aug. 1993.

[14] B. Tilma *et al.,* "Integrated tunable quantum-dot laser for optical coherence tomography in the 1.7 μm wavelength region," *IEEE J. Quant. Electron.*, vol. 48, no. 2, pp. 87–98, Feb. 2012.

[15] B. Tilma *et al.,* "InP-based monolithically integrated tunable wavelength filters in the 1.6–1.8 μm wavelength region for tunable laser purposes," *J. Lightw. Technol.*, vol. 29, no. 18, pp. 2818–2830, Sep. 2011.

[16] J. C. Hulme, J. K. Doylend, and J. E. Bowers, "Widely tunable Vernier ring laser on hybrid silicon," *Opt. Exp.*, vol. 21, no. 17, pp. 19718–19722, Aug. 2013.

[17] A. Le Liepvre *et al.,* "Widely wavelength tunable hybrid III-V/silicon laser with 45 nm tuning range fabricated using a wafer bonding technique," in *Proc. IEEE 9th Int. Conf. GFP*, Aug. 2012, pp. 54–56.

[18] M. Smit *et al.,* "An introduction to InP-based generic integration technology," *Semicond. Sci. Technol.*, vol. 29, no. 8, Jun. 2014, Art. ID. 083001.
[19] SMART Photonics. [Online]. Available: http://www.smartphotonics.nl/
[20] Joint European Platform for InP-Based Photonic Integrated Components and Circuits. [Online]. Available: http://www.jeppix.eu/
[21] S. Latkowski, M. Smit, and E. A. J. M. Bente, "Integrated tunable semiconductor laser geometry based on asymmetric Mach–Zehnder interferometers for gas sensing applications," in *Proc. 17th Annu. Symp. IEEE Photon. Soc. Benelux Chapter*, 2012, pp. 199–202. [Online]. Available: http://www.tue.nl/publicatie/ep/p/d/ep-uid/278037/
[22] S. Latkowski, T. D. Vries, L. Augustin, S. Meint, and E. Bente, "A monolithically integrated tunable single longitudinal mode extended cavity ring laser using intracavity Mach–Zehnder interferometers," in *Proc. 18th Annu. Symp. IEEE Photon. Benelux Chapter*, Eindhoven, The Netherlands, Nov. 2013, pp. 97–100.
[23] E. Bente, S. Latkowski, T. de Vries, and M. Smit, "Widely tunable monolithically integrated lasers using intracavity Mach–Zehnder interferometers," in *Proc. IEEE 16th ICTON*, Jul. 2014, pp. 1–4.
[24] S. Calvez, X. Rejeaunier, P. Mollier, J.-P. Goedgebuer, and W. T. Rhodes, "Erbium-doped fiber laser tuning using two cascaded unbalanced Mach–Zehnder interferometer as intracavity filter: Numerical analysis and experimental confirmation," *J. Lightw. Technol.*, vol. 19, no. 6, pp. 893–898, Jun. 2001.
[25] L. A. Coldren, S. W. Corzine, and M. L. Mashanovitch, *Diode Lasers and Photonic Integrated Circuits*. New York, NY, USA: Wiley, Mar. 2012.
[26] J. Mendoza-Alvarez *et al.,* "Analysis of depletion edge translation lightwave modulators," *J. Lightw. Technol.*, vol. 6, no. 6, pp. 793–808, Jun. 1988.
[27] J.-F. Vinchant, J. Cavailles, M. Erman, P. Jarry, and M. Renaud, "InP/GaInAsP guided-wave phase modulators based on carrier-induced effects: Theory and experiment," *J. Lightw. Technol.*, vol. 10, no. 1, pp. 63–70, Jan. 1992.
[28] PhI Circuit Simulation—InP PIC Simulation Software. [Online]. Available: https://sites.google.com/site/inplaserseb/phi-circuit-simulation
[29] PICWave—Photonic IC (PIC)/Laser Diode/SOA Simulator for Active and Passive Devices. [Online]. Available: http://www.photond.com/products/picwave.htm
[30] PhoeniX Software—Solutions for Micro and Nano Technologies. [Online]. Available: http://www.phoenixbv.com/
[31] T. Okoshi, K. Kikuchi, and A. Nakayama, "Novel method for high resolution measurement of laser output spectrum," *Electron. Lett.*, vol. 16, no. 16, pp. 630–631, Jul. 1980.
[32] Y. Akulova *et al.,* "Widely tunable electroabsorption-modulated sampled-grating DBR laser transmitter," *IEEE J. Sel. Topics Quant. Electron.*, vol. 8, no. 6, pp. 1349–1357, Nov. 2002.
[33] A. Ward *et al.,* "Widely tunable DS-DBR laser with monolithically integrated SOA: Design and performance," *IEEE J. Sel. Topics Quant. Electron.*, vol. 11, no. 1, pp. 149–156, Jan. 2005.
[34] D. Lavery *et al.,* "Digital coherent receivers for long-reach optical access networks," *J. Lightw. Technol.*, vol. 31, no. 4, pp. 609–620, Feb. 2013.
[35] K. Nakagawa, M. de Labachelerie, Y. Awaji, and M. Kourogi, "Accurate optical frequency atlas of the 1.5 μm bands of acetylene," *J. Opt. Soc. Amer. B, Opt. Phys.*, vol. 13, no. 12, pp. 2708–2714, Dec. 1996.